

RESEARCH ARTICLE

Syncollin is an antibacterial polypeptide

Rosie A. Waters¹ | James Robinson² | J. Michael Edwardson¹ 

¹Department of Pharmacology, University of Cambridge, Cambridge, UK

²Mechanistic Biology and Profiling, Discovery Sciences, R&D, AstraZeneca, Cambridge, UK

Correspondence

J. Michael Edwardson, Department of Pharmacology, University of Cambridge, Tennis Court Road, Cambridge CB2 1PD, UK.
Email: jme1000@cam.ac.uk

Funding information

AstraZeneca; David James Studentship, Department of Pharmacology, University of Cambridge

Abstract

Syncollin is a 16-kDa protein found predominantly in the zymogen granules of pancreatic acinar cells, with expression at lower levels in intestinal epithelial cells and neutrophils. Here, we used Strep-tagged syncollin isolated from the supernatant of transiently transfected mammalian cells to test the hypothesis that syncollin has antibacterial properties, which might enable it to play a role in host defence in the gut and possibly elsewhere. We show that syncollin is an exceptionally thermostable protein with a circular dichroism spectrum consistent with a predominantly beta-sheet structure. Syncollin binds to bacterial peptidoglycan and restricts the growth of representative Gram-positive (*Lactococcus lactis*) and Gram-negative (*Escherichia coli*) bacteria. Syncollin induces propidium iodide uptake into *E. coli* (but not *L. lactis*), indicating permeabilisation of the bacterial membrane. It also causes surface structural damage in both *L. lactis* and *E. coli*, as visualised by scanning electron microscopy. We propose that syncollin is a previously unidentified member of a large group of antimicrobial polypeptides that control the gut microbiome.

Take Aways

- Syncollin is a 16-kDa protein found in pancreatic zymogen granules.
- Syncollin is highly thermostable and has a predominantly beta-sheet structure.
- Syncollin binds peptidoglycan and restricts the growth of *L. lactis* and *E. coli*.
- Syncollin causes propidium iodide uptake into *E. coli* (but not *L. lactis*).
- Syncollin causes surface structural damage in both *L. lactis* and *E. coli*.

KEYWORDS

antibacterial polypeptide, pancreatic zymogen granule, peptidoglycan, syncollin

Abbreviations: BSA, bovine serum albumin; CD, circular dichroism; CHAPS, 3-[[3-(cholamidopropyl)dimethylammonio]-1-propanesulfonate]; DMEM, Dulbecco's modified Eagle's medium; EM, electron microscopy; GST, glutathione S-transferase; HEPES, 4-(2-hydroxyethyl)-1-piperazineethanesulfonic acid; HBS, HEPES-buffered saline; OD, optical density; PBS, phosphate-buffered saline; SDS-PAGE, sodium dodecyl sulfate–polyacrylamide gel electrophoresis; ZG, zymogen granule.

This is an open access article under the terms of the Creative Commons Attribution License, which permits use, distribution and reproduction in any medium, provided the original work is properly cited.

© 2021 The Authors. *Cellular Microbiology* published by John Wiley & Sons Ltd.

1 | INTRODUCTION

Syncollin is a 16-kDa protein that was originally isolated from the pancreatic zymogen granule (ZG; Edwardson, An, & Jahn, 1997). The protein is present free within the ZG lumen and also tightly associated with the luminal leaflet of the ZG membrane (An, Hansen, Hodel, Jahn, & Edwardson, 2000). Syncollin is able to oligomerise, and atomic force microscopy images of the protein bound to lipid bilayers reveal doughnut-shaped structures (Geisse, Wäsle, Saslowsky, Henderson, &

Edwardson, 2002). Consistent with this ‘pore-like’ appearance, syncollin is able to permeabilise both the erythrocytes (Wäsle, Hays, Rhodes, & Edwardson, 2004) and liposomes (Geisse et al., 2002).

Syncollin is expressed not only in the exocrine pancreas but also in the gut and the spleen (Edwardson et al., 1997; Tan & Hooi, 2000). In the rat gut, it is present principally in epithelial cells lining the proximal duodenum and the colon. Expression of syncollin in the gut is almost undetectable until rats begin suckling, when expression rises rapidly; further, syncollin expression falls upon starvation and then rebounds upon refeeding (Tan & Hooi, 2000). Syncollin is also found in azurophilic granules of human neutrophils and is secreted from these cells upon stimulation (Bach et al., 2006). These observations suggest that syncollin might play a role in host defence, as first proposed by Bach et al. (2006).

There is evidence for the involvement of syncollin in a number of disease states, particularly related to the gut. For instance, syncollin expression was found to be strongly down-regulated in the colon when a bacterial suspension was administered to germ-free mice (Fukushima, Funayama, Ogawa, Takahashi, & Sasaki, 2003) and in mice with chemically induced colitis-associated cancer (Li et al., 2014). In addition, syncollin mRNA is significantly reduced in intestinal epithelia taken from patients with ulcerative colitis (but not Crohn's disease; Fukushima et al., 2003). Finally, syncollin levels are significantly elevated in both pancreatic juice (Makawita et al., 2011) and serum taken from pancreatic cancer patients (Makawita et al., 2013), suggesting that it might be a useful pancreatic cancer biomarker.

Since syncollin is a component of the pancreatic juice and is implicated in a number of gut disease states, it is tempting to speculate that it may be active in the gut. We set out to test this hypothesis. Here, we show that syncollin is a very stable protein, consistent with a function in the pancreatic juice. It binds to bacterial peptidoglycan and restricts the growth of representative Gram-positive and Gram-negative bacteria, reducing the viability of the latter. We also show that syncollin causes profound structural changes to the surface of bacteria. We propose that syncollin might be a previously unidentified member of a large group of antimicrobial polypeptides that control the gut microbiome. Further, the fact that syncollin is known to be secreted in response to activation of human neutrophils suggests that it might be involved in host defence more widely.

2 | RESULTS

2.1 | Purification of syncollin-Strep

tsA-201 cells were transfected with a syncollin-Strep construct in pcDNA3.1, and syncollin-Strep was purified from cell supernatants using the Strep-Tactin XT™ system. Following biotin elution of syncollin from Strep-Tactin XT™ beads, the protein ran at ~20 kDa and appeared as a triple band on silver-stained gels and immunoblots (Figure 1a). Analysis of these bands by mass spectroscopy indicated that all three are syncollin. We could not find any evidence for post-translational modification of the protein. We therefore propose that

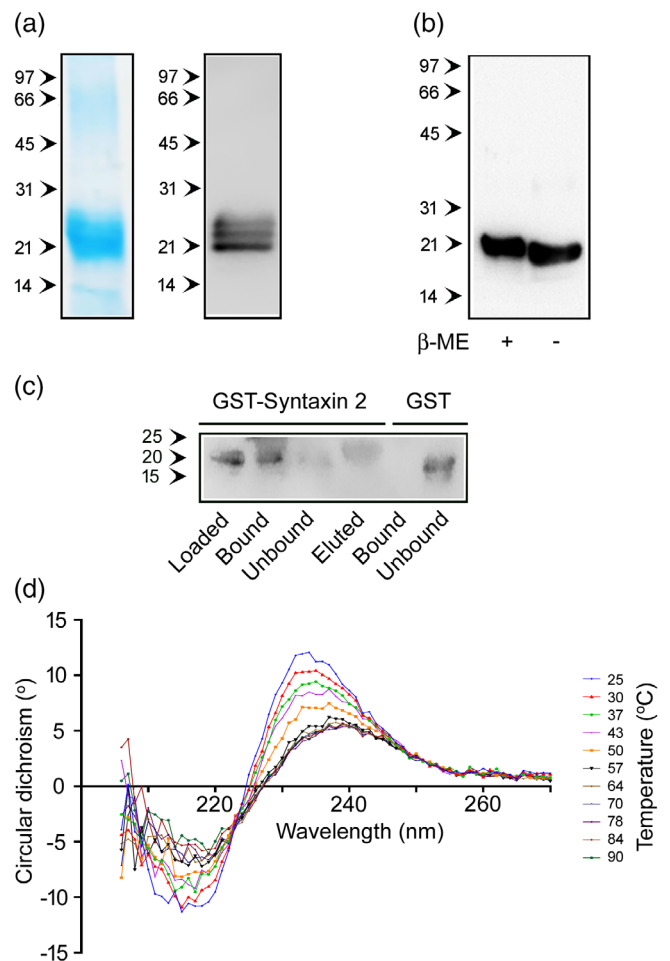


FIGURE 1 Isolation and characterization of syncollin-Strep. (a) Analysis of isolated syncollin-Strep by sodium dodecyl sulfate–polyacrylamide gel electrophoresis (SDS-PAGE) followed by Coomassie blue staining (left) or immunoblotting (right). Molecular mass markers (in kDa) are indicated. (b) Immunoblot of syncollin-Strep after SDS-PAGE in the absence and presence of β -mercaptoethanol (10% [v/v]). (c) Interaction of syncollin-Strep with syntaxin 2. Syncollin-Strep was incubated with either glutathione S-transferase (GST)-syntaxin 2, or GST alone, bound to glutathione-Sepharose™, and loaded, bound and unbound samples were analysed by immunoblotting. Syncollin-Strep eluted from GST-syntaxin 2 with free reduced glutathione (15 mM) was also analysed. Since the polyclonal anti-syncollin antibody used also recognises GST, only the region of the blot where syncollin migrates is shown, for clarity. (d) Circular dichroism (CD) spectra of syncollin-Strep at various temperatures. The results presented in (a) are representative of those from ~60 syncollin-Strep purifications; results in (b–d) are representative of those from two experiments

the three bands represent differentially folded (and possibly differentially disulfide bonded) forms.

2.2 | Syncollin quality control

As a quality control measure, the purified syncollin-Strep was checked for two properties known to be hallmarks of native syncollin – the

presence of disulfide bonds (An et al., 2000) and the ability to bind to syntaxin 2 (Edwardson et al., 1997). Syncollin was analysed by sodium dodecyl sulfate–polyacrylamide gel electrophoresis (SDS-PAGE) in either the presence or absence of β -mercaptoethanol followed by immunoblotting. The immunoblot (Figure 1b) shows that the protein migrated more slowly in the presence than in the absence of β -mercaptoethanol, consistent with unfolding upon reduction of its disulfide bonds. As shown in Figure 1c, syncollin-Strep bound to glutathione S-transferase (GST)-syntaxin 2 (but not to GST alone) attached to GSH-Sepharose™ beads and could be eluted upon addition of reduced glutathione. Hence, at least two key characteristics of the native protein are retained in purified recombinant syncollin-Strep.

Following secretion into the pancreatic juice, syncollin will enter an environment rich in proteolytic activity. One might expect, therefore, that its structure would be highly stable. To test this hypothesis, the thermal stability of the protein was assessed using circular dichroism (CD) spectroscopy. The CD spectrum of syncollin-Strep (10 μ M in 10 mM sodium phosphate, pH 8.0 containing 0.1% [w/v] CHAPS), had two peaks: a negative peak at approximately 218 nm and a positive peak at approximately 234 nm (Figure 1d), consistent with a predominantly beta-sheet structure. When the protein was subjected to a temperature ramp up to 90°C, both peaks were reduced in amplitude, although complete unfolding did not occur, indicating that the protein does indeed have a very high thermal stability.

2.3 | Syncollin binds to bacterial peptidoglycan

To explore a potential role for syncollin in host defence, we first examined whether syncollin-Strep binds to bacterial peptidoglycan. Syncollin-Strep or BSA was incubated with peptidoglycan (320 μ g), and the peptidoglycan was pelleted by centrifugation. The majority of the syncollin-Strep was found in the pellet, whereas all of the BSA remained in the supernatant (Figure 2). In the absence of peptidoglycan, syncollin-Strep remained in the supernatant. These results suggest that syncollin is likely to bind to bacterial cell walls.

2.4 | Syncollin restricts bacterial growth

To assess whether there is a functional effect of syncollin binding to bacteria, we determined the effect of various concentrations of syncollin-Strep on the growth of Gram-positive *Lactococcus lactis* and Gram-negative *Escherichia coli*. Increasing concentrations of syncollin-Strep caused a shift to the right of the *L. lactis* growth curve (optical density (OD) 600 nm versus time), reaching a >200-min time delay to reach the exponential phase at 163 μ g/ml (8 μ M) syncollin-Strep (Figure 3a). The T_{50} value (the time taken for the curve to reach half of its maximal OD) became significantly different from control at this concentration (Figure 3b). Further, both the span and the Hill slope of the growth curve were also reduced at 163 μ g/ml syncollin-Strep (Figure 3c,d).

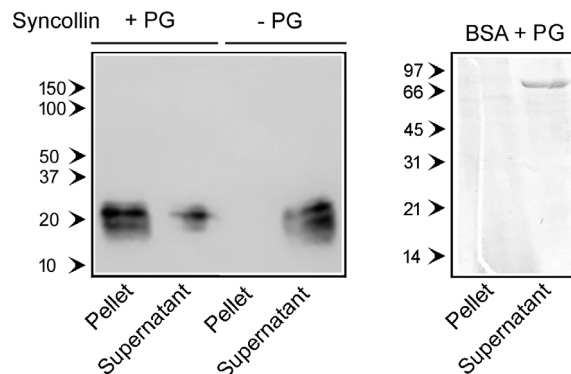


FIGURE 2 Interaction of syncollin-Strep with peptidoglycan. Syncollin-Strep and bovine serum albumin (BSA) (33 μ g in both cases) were incubated with insoluble peptidoglycan (PG; 320 μ g). In a control experiment, syncollin-Strep was also incubated without PG. The PG was then pelleted by centrifugation, and the presence of protein in the pellet and the supernatant was determined by either immunoblotting (for syncollin-Strep) or Coomassie Blue staining (for BSA). Molecular mass markers (in kDa) are indicated. The results are representative of those from five experiments

In contrast to the results for *L. lactis*, syncollin-Strep did not shift the growth curve for *E. coli*, (Figure 4a), and the T_{50} value was unaffected at all concentrations of the protein (Figure 4b). Syncollin-Strep did, however, significantly reduce the span of the *E. coli* growth curves at 81.5 and 163 μ g/ml (Figure 4c). The Hill slope of the curve was unaffected at all concentrations (Figure 4d). Hence, syncollin produces different effects on the growth of Gram-positive and Gram-negative bacteria.

As a control for the presence of protein in the growth medium, the effects of soybean trypsin inhibitor and ribonuclease A on the growth of *L. lactis* and *E. coli* were tested. As shown in Figure 5, neither protein shifted the growth curve for *L. lactis* (Figure 5a) or reduced the span of the curve for *E. coli* (Figure 5b), under conditions in which syncollin-Strep again caused clear effects, indicating that syncollin specifically restricts the growth of both Gram-positive and Gram-negative bacteria.

2.5 | Interactions between syncollin and antibiotics

The effects of syncollin-Strep (110 μ g/ml) on the growth of *L. lactis* in combination with the antibiotics ampicillin (bactericidal) and tetracycline (bacteriostatic) were assessed (Figure 6a,b). The concentrations of the two antibiotics (0.05 and 2 μ g/ml, respectively) were chosen so as to produce a clear effect on bacterial growth but not to inhibit growth completely. As shown in Figure 6c, syncollin-Strep, ampicillin and tetracycline, when added alone, all failed to cause a significant reduction in the span of the growth curve for *L. lactis*. However, syncollin-Strep in combination with either ampicillin or tetracycline did significantly reduce the span. None of the treatments used, either alone or in combination, caused a significant effect on the T_{50} of the

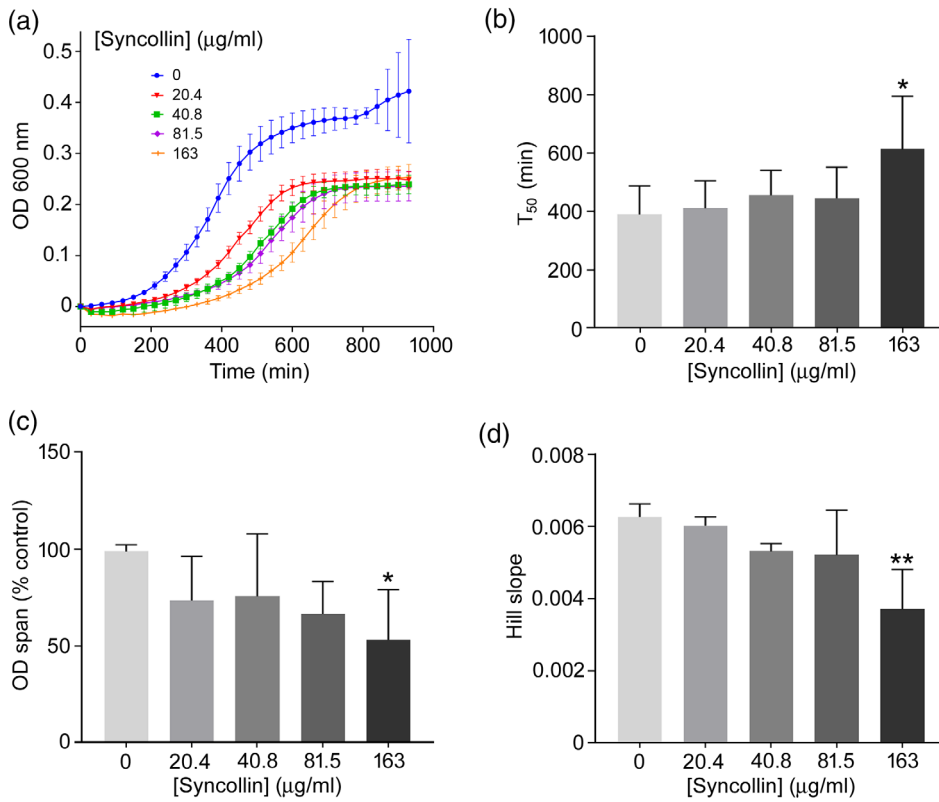


FIGURE 3 Effect of syncollin-Strep on the growth of *Lactococcus lactis*. (a) Bacteria were incubated with various concentrations of syncollin-Strep and optical density (OD) at 600 nm was measured every 30 min over a ~20-hr time-course. Error bars are SD ($n = 3$). (b–d) Effect of syncollin-Strep, at various concentrations, on (b) T_{50} , the time taken for the growth curve to reach half of its maximal OD, (c) the increase in OD over the course of the curve (span), and (d) the Hill slope of the curve. Data are from five experiments. Error bars are SD. * $p < .05$; ** $p < .01$, compared with buffer control (one-way Analysis of Variance [ANOVA] with Dunnett's multiple comparisons)

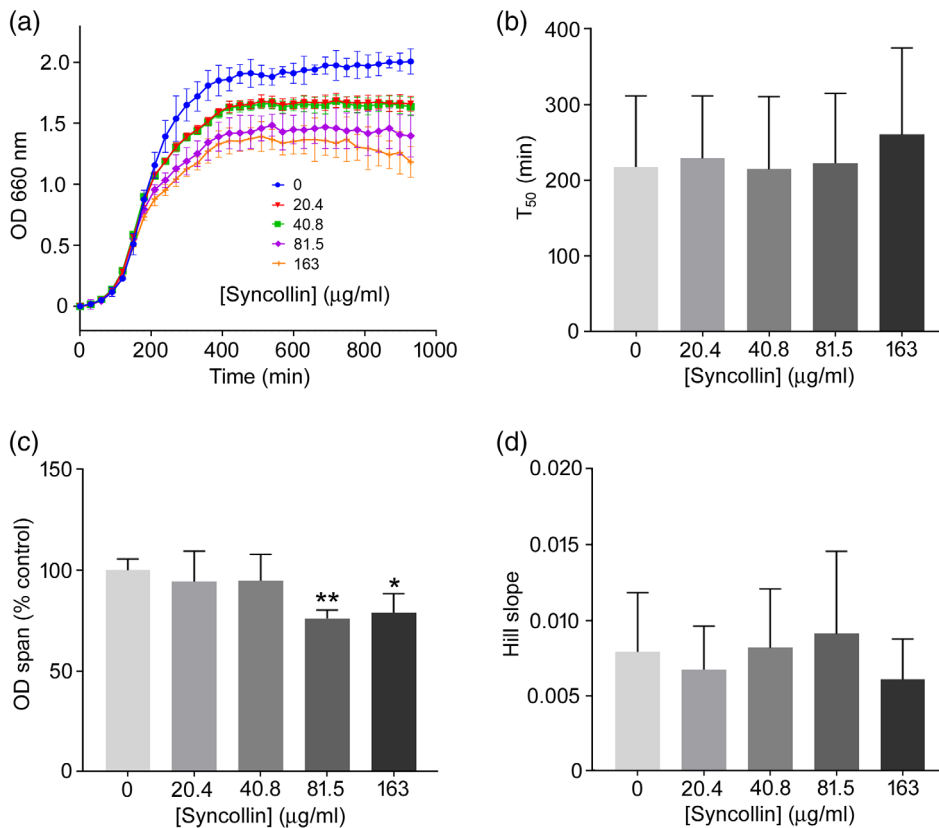


FIGURE 4 Effect of syncollin-Strep on the growth of *Escherichia coli*. (a) Bacteria were incubated with various concentrations of syncollin-Strep and optical density (OD) at 660 nm was measured every 30 min over a ~20-hr time-course. Error bars are SD ($n = 3$). (b–d) Effect of syncollin-Strep, at various concentrations, on (b) T_{50} , the time taken for the growth curve to reach half of its maximal OD, (c) the increase in OD over the course of the curve (span), and (d) the Hill slope of the curve. Data are from five experiments. Error bars are SD. * $p < .05$; ** $p < .01$, compared with buffer control (one-way Analysis of Variance [ANOVA] with Dunnett's multiple comparisons)

growth curve (Figure 6d). The additive effects of syncollin-Strep and ampicillin are of particular interest because a bacteriostatic agent would be expected to abrogate rather than enhance the effect of the

bactericidal ampicillin. This result suggests that syncollin-Strep might be causing its own killing effect in addition to that brought about by ampicillin.

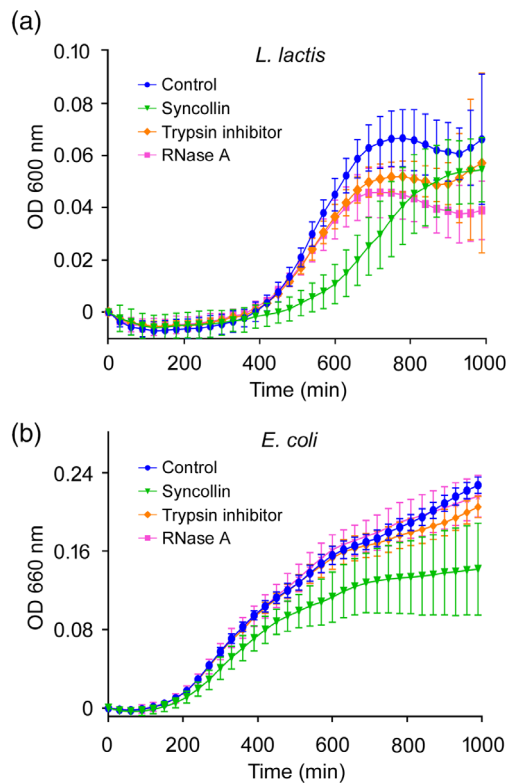


FIGURE 5 Control for the presence of protein in the incubation medium. Bacterial growth curves for *Lactococcus lactis* (a) and *Escherichia coli* (b) were generated in the presence of syncollin-Strep, soybean trypsin inhibitor and RNase A (all at 300 $\mu\text{g}/\text{ml}$). Optical density (OD) at 600 nm (*L. lactis*) or 660 nm (*E. coli*) was measured every 30 min over a ~ 20 -hr time-course. Error bars are SD ($n = 5$). The results are representative of those from three experiments

When added to *E. coli*, both ampicillin and tetracycline produced a substantial flattening of the growth curve; in contrast, syncollin-Strep was without obvious effect (Figure S1a,b). The reduction in the span of the curve caused by both antibiotics was highly significant, and the combination of syncollin-Strep with either antibiotic did not cause a further reduction (Figure S1c,d).

2.6 | Syncollin reduces the viability of *E. coli*

Following our observations of effects on bacterial growth, we next assessed bacterial viability after treatment with syncollin-Strep, ampicillin and tetracycline through the uptake of propidium iodide, which is taken up only by dead cells. Bacteria were sampled either in log phase or plateau phase and incubated in a solution containing propidium iodide (1 $\mu\text{g}/\text{ml}$). 4',6'-Diamidino-2-phenylindole dihydrochloride (DAPI) (1 $\mu\text{g}/\text{ml}$) was used to stain all of the bacterial cells. As shown in Figure S2, in log phase, none of the three treatments caused a significant increase in the numbers of propidium iodide-positive (red) cells for either *L. lactis* or *E. coli*. In contrast, in the plateau phase, ampicillin, but not tetracycline, caused significant permeabilisation of both *L. lactis* and *E. coli* cells (Figure 7). Interestingly, syncollin-Strep caused significant permeabilisation of *E. coli* but

not *L. lactis*. Further, both syncollin-Strep and ampicillin caused an increase in the proportion of filamentous forms of *E. coli* (arrows, Figure 7a), which are typically seen under conditions of cell stress (Murashko & Lin-Chao, 2017). The permeabilising effect of syncollin-Strep specifically on *E. coli* is consistent with the suggestion (above) that the protein acts differentially on Gram-positive and Gram-negative bacteria.

2.7 | Scanning electron microscopy shows structural changes in response to syncollin treatment

To assess the effects of syncollin on the surfaces of *L. lactis* and *E. coli* bacteria, we turned to scanning electron microscopy (SEM). Bacteria were incubated in either buffer alone or in buffer containing syncollin-Strep (0.3 mg/ml) before imaging. As shown in Figures 8, S3 and S4, control images reveal smooth-surfaced spherical (*L. lactis*) and rod-shaped structures (*E. coli*). In contrast, bacteria treated with syncollin-Strep were mis-shapen and rough-surfaced. These results indicate profound structural changes to the bacteria brought about by syncollin-Strep treatment, in parallel with the membrane permeabilisation described above. Incubation with trypsin inhibitor or ribonuclease A caused only a modest increase in the surface roughness of both types of bacteria, consistent with their lack of significant effect on bacterial growth.

3 | DISCUSSION

We have shown here that syncollin hinders the growth of Gram-positive (*L. lactis*) and Gram-negative (*E. coli*) bacteria, reducing the viability of the latter in the plateau phase of growth. Syncollin also causes obvious structural damage to the bacterial capsule in both *L. lactis* and *E. coli*. Syncollin has two properties that are likely to be involved in its antibacterial activity – the ability to bind to peptidoglycan, as demonstrated in this study, and the ability to permeabilise biological membranes (Wäsle et al., 2004) and lipid bilayers (Geisse et al., 2002). We suggest that the slowing of the growth of *L. lactis* (but not *E. coli*) in log phase might be caused primarily through binding to the exposed peptidoglycan-based cell wall in the former, whereas the permeabilisation of the *E. coli* (but not *L. lactis*) in the plateau phase might be caused by an action of syncollin on the membranes of the Gram-negative bacterium. Further studies will be required to confirm this suggestion.

Syncollin-knockout mice are viable and fertile, although gut physiology and sensitivity to bacterial challenge have not been addressed. Given that a plethora of antibacterial polypeptides are known to be secreted into the gut (see below), it is perhaps unlikely that the absence of just one (syncollin) would cause an obvious gut phenotype. Signs of abnormality in the pancreas of the knockout mice were detected, including an increase in the numbers of ZGs within the acinar cells and a reduction in the number of individual exocytotic events (Wäsle et al., 2005). Could it be that a component of the exocytotic machinery ‘moonlights’ as an antibacterial protein? At present, we

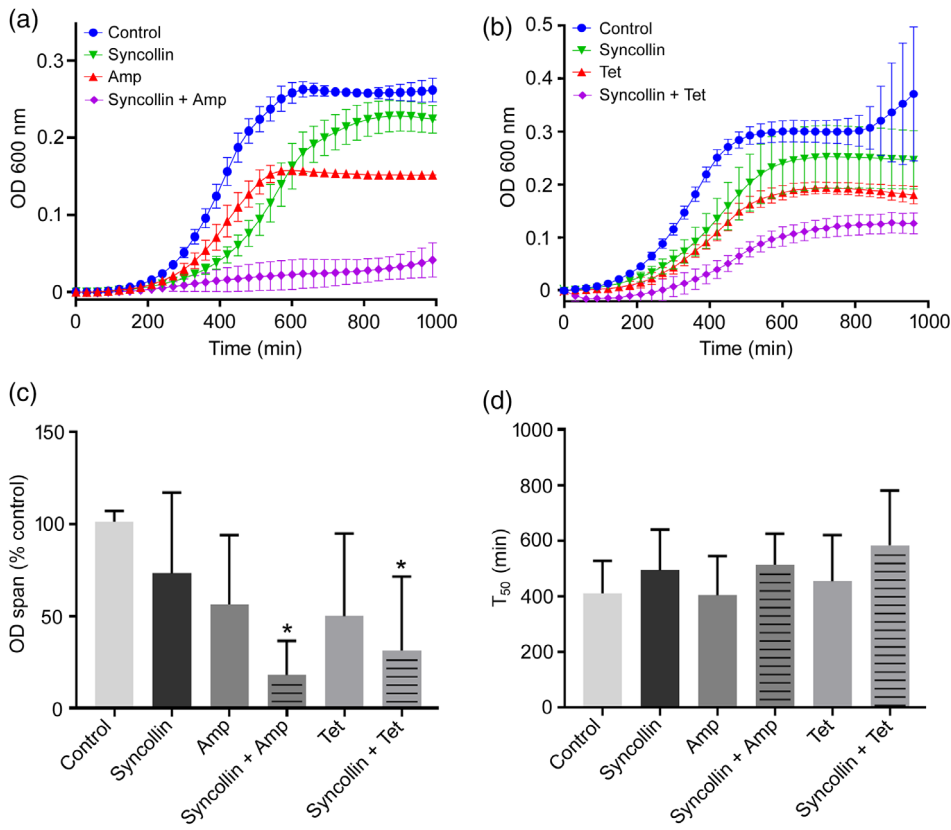


FIGURE 6 Effect of syncollin-Strep on the growth of *Lactococcus lactis* in combination with antibiotics. (a) Bacteria were incubated with buffer alone, syncollin-Strep (110 $\mu\text{g}/\text{ml}$), ampicillin (0.05 $\mu\text{g}/\text{ml}$) or syncollin-Strep plus ampicillin, and optical density (OD) at 600 nm was measured every 30 min over a ~ 20 -hr time-course. Error bars are SD ($n = 4$). (b) Bacteria were incubated with buffer alone, syncollin-Strep (110 $\mu\text{g}/\text{ml}$), tetracycline (2 $\mu\text{g}/\text{ml}$) or syncollin-Strep plus tetracycline, and OD at 600 nm was measured every 30 min over a ~ 20 -hr time-course. Error bars are SD ($n = 4$). (c,d) Effect of syncollin and antibiotics, alone and in combination, on (c) the span of the curve and (d) the T_{50} of the curve. Data are from five experiments. Error bars are SD. * $p < .05$, compared with buffer control (one-way Analysis of Variance [ANOVA] with Tukey's multiple comparisons)

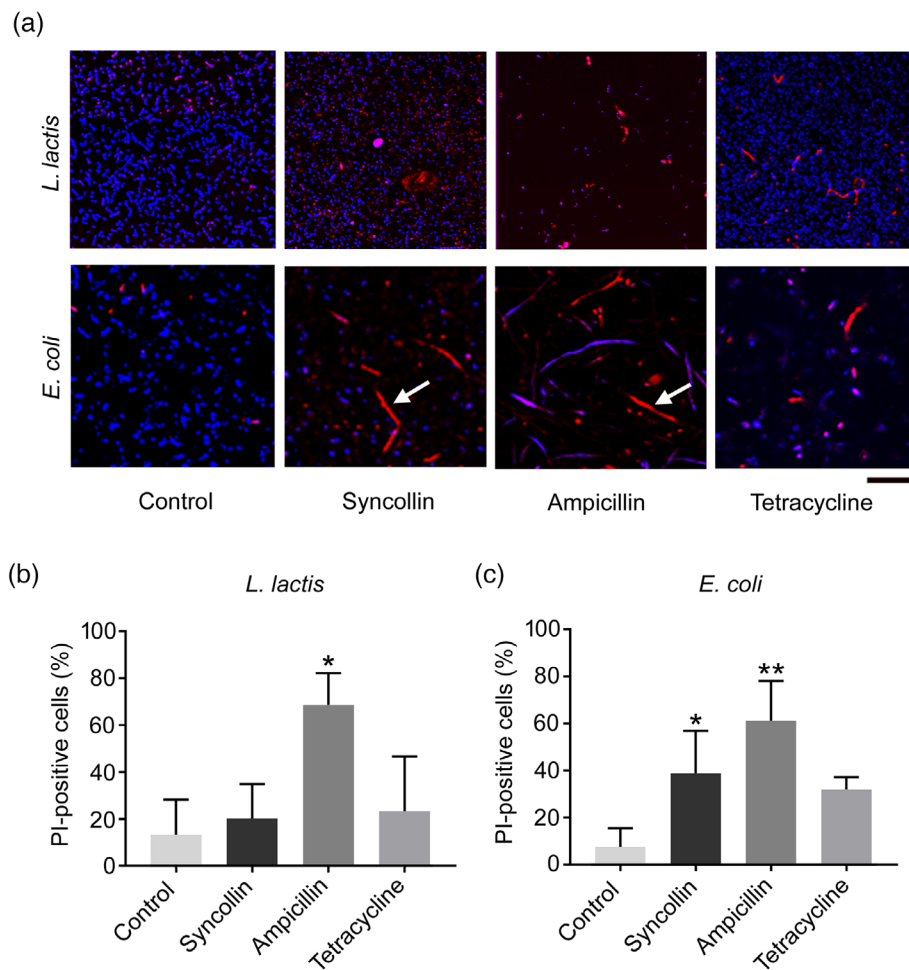
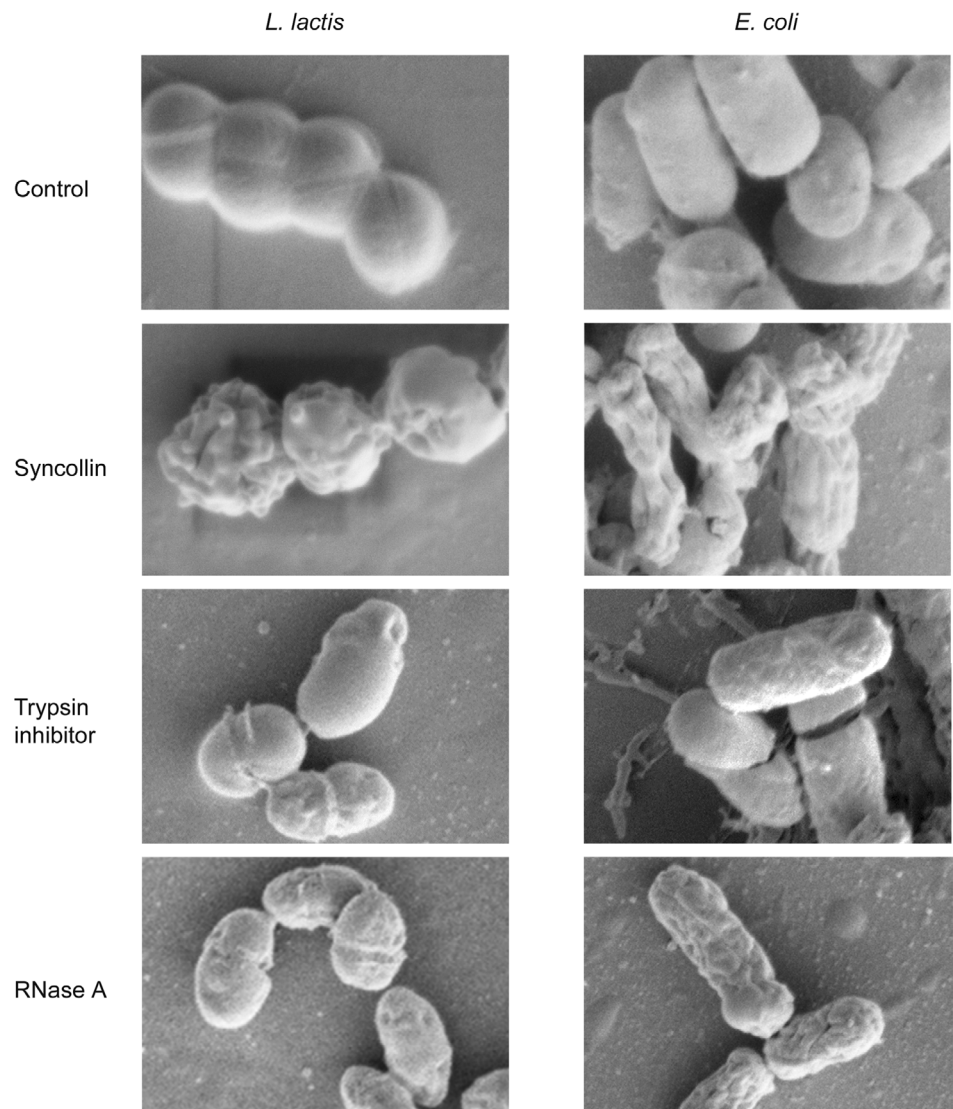


FIGURE 7 Effect of syncollin-Strep on bacterial viability in the plateau phase of growth. Bacteria were incubated with buffer alone, syncollin-Strep (300 $\mu\text{g}/\text{ml}$), ampicillin (0.05 $\mu\text{g}/\text{ml}$) or tetracycline (2 $\mu\text{g}/\text{ml}$). When bacteria reached the early plateau phase of growth, they were incubated in phosphate-buffered saline (PBS) containing propidium iodide (1 $\mu\text{g}/\text{ml}$; red) and 4',6'-diamidino-2-phenylindole dihydrochloride (DAPI) (1 $\mu\text{g}/\text{ml}$; blue) before imaging by confocal microscopy. (a) Representative images for various conditions. Filamentous forms of *Escherichia coli* are indicated by arrows. Scale bar, 20 μm . (b) Quantitation of results from three experiments. * $p < .05$; ** $p < .01$, compared with buffer control (one-way ANOVA with Dunnett's multiple comparisons)

FIGURE 8 Scanning electron microscopy (SEM) analysis of the effects of syncollin-Strep and control proteins on bacterial structure. Bacteria were incubated in either buffer alone or in buffer containing protein (0.3 mg/ml) before SEM imaging. Scale bar, 1 μ m. The results are representative of those from three experiments



cannot rule this out, although it is worth pointing out that compound exocytosis continues at a reduced rate in the knockout mice, rather than being completely abolished. Further, compound exocytosis occurs in several other cell types (e.g., mast cells) that do not express syncollin. It is clear that syncollin is a major component of the protein matrix lining the luminal surface of the ZG membrane. It is therefore possible that its absence in the knockout mouse causes structural abnormalities that perturb the function of the membrane during exocytosis.

Intriguingly, syncollin shares features with other small antimicrobial polypeptides that are known to play roles in host defence in the gut, including ZG16p, RegIII and members of the defensin family. These features include a predominantly beta-sheet structure, the presence of intramolecular disulfide bonds, and in some cases, an ability to form homo-oligomers. ZG16p, like syncollin, is located on the luminal surface of the pancreatic ZG membrane (Kalus et al., 2002). It has a predominantly beta-sheet structure and contains a single intramolecular disulfide bond (Kanagawa et al., 2011). Members of the

regenerating islet-derived (Reg) protein family also adopt a predominantly beta-sheet structure. The family member RegIII γ is secreted into the intestinal lumen, where it has antibacterial actions (Shin & Seeley, 2019). RegIII α is capable of forming hexamers on bacterial membranes, resulting in the formation of a transmembrane pore and membrane leakiness (Mukherjee et al., 2014). Defensins are small proteins (3–4 kDa), which have a predominantly beta-sheet structure (Min et al., 2017), and six disulfide-bonded cysteines. Defensins, like RegIII α , are able to form pores and permeabilise bacterial membranes.

As mentioned above, syncollin is also expressed in (and secreted from) neutrophils (Bach et al., 2006), again consistent with a role in host defence. Indeed, the authors of this previous paper speculated that syncollin might have an antibacterial effect but were unable to demonstrate this property. We suggest that this failure might have been a result of the elaborate method used to prepare native syncollin (removal from the ZG membrane at high pH followed by selective precipitation in an aggregated state after dialysis to neutral pH; An et al., 2000).

In conclusion, given the structural similarities between the properties of syncollin and those of other known antimicrobial proteins, together with the functional properties reported here, we propose that syncollin is a previously unidentified member of the antimicrobial protein superfamily. It is known that pancreatic juice has antibacterial activity (Rubinstein et al., 1985), which is likely to be important not only for the control of the bacterial flora of the upper intestine but also for protection of the pancreas itself from infection. Structural studies are currently underway to shed light on how syncollin folds, oligomerises and interacts with its bacterial targets.

4 | EXPERIMENTAL PROCEDURES

4.1 | Syncollin construct

All enzymes, buffers and reagents were from NEB, unless otherwise stated. A double-Strep-II tag was added to the syncollin sequence in order to facilitate its isolation through binding to Strep-Tactin XT™ beads (IBA). A linker and a TEV-protease site were first added immediately downstream of the syncollin sequence. To achieve this, syncollin DNA was amplified by polymerase chain reaction (PCR) to include restriction enzyme sites for *AgeI* and *NotI* using the forward primer: 5'-ATAACCGGTATGTCCCCGCTGTGCCTGCTGTTGC-3' and the reverse primer: 5'-ATAGCGGCCGCGCCCTGGAAGTACAGTTCTCGCCACCATAGCACTTGCAGTA-3'. Two Strep-II tags were then inserted downstream of the TEV site. These were amplified by PCR from a vector kindly donated by Mekdes Debela (Department of Biochemistry, University of Cambridge), using the forward primer: 5'-ATAGCGGCCGTTGGAGTCATCCT-3' and the reverse primer: 5'-ATACCTGCAGGTCATCACTTCTCAAAGT-3' to incorporate *NotI* and *SbfI* restriction enzymes sites around the Strep-II tags for insertion downstream of syncollin. The syncollin-Strep sequence was cloned into a pcDNA3.1 backbone using the primers 5'-AATAAGCTTATGTCCCCGCTGTGCCTGCTGTTGCT-3' and 5'-AATACCGGTTTCATCACTTCTCAAAGTGTGGATGGG-3' to incorporate *HindIII* and *AgeI* restriction sites. Syncollin-Strep was then ligated into the *HindIII*- and *AgeI*-cleaved pcDNA3.1 backbone. The sequence of the final construct was confirmed by Sanger sequencing.

4.2 | Syncollin purification

tsA-201 cells (a sub-clone of human embryonic kidney-293 cells stably expressing the SV40 large T-antigen) were grown in high-glucose Dulbecco's modified Eagle's medium (DMEM; Sigma) containing 10% (v/v) fetal bovine serum and 1% (w/v) penicillin/streptomycin (Thermo) at 37°C in an atmosphere of 5% (v/v) CO₂/air. Cells were transfected at 70–80% confluence using polyethyleneimine (Sigma) and 19 µg DNA for each 175 cm² flask. (A typical purification used 20 flasks.) Transfected cells were incubated for 96 hr to allow protein expression. The cells were then centrifuged at 100g for 4 min, and the supernatant was incubated with a 1:100 volume of Strep-Tactin XT™

beads for 3 hr at 4°C. All subsequent steps were carried out at 4°C. Beads were pelleted by centrifugation for 5 min at 21,000g, and the supernatant was discarded. The beads were resuspended in wash buffer (10 mM sodium phosphate, pH 8.0) supplemented with cOmplete™ protease inhibitors (Sigma) and 0.1% (w/v) 3-[(3-cholamidopropyl)dimethylammonio]-1-propanesulfonate (CHAPS) and loaded into an Econo-Pac™ disposable chromatography column (BioRad). The column was washed with 20 column volumes, and bound protein was eluted using 7 x 2 column volumes of wash buffer containing 50 mM biotin. All fractions were analysed using SDS-PAGE followed by either Coomassie Blue staining or immunoblotting using a rabbit polyclonal anti-syncollin antibody (Hodel & Edwardson, 2000). Immunopositive bands were detected using a horseradish peroxidase-conjugated goat anti-rabbit antibody (BioRad) and enhanced chemiluminescence (Thermo). Syncollin-Strep was concentrated to 5 mg/ml (250 µM) using 10-kDa molecular mass cut-off concentrators (Amicon). After use, the Strep-Tactin XT™ beads were regenerated for further use through addition of 4'-hydroxyazobenzene-2-carboxylic acid, which removes the bound biotin.

4.3 | Syncollin quality control

To check for the presence of disulfide bonds, purified syncollin-Strep was analysed by SDS-PAGE in the presence or absence of β-mercaptoethanol, followed by assessment of band migration on an immunoblot.

To check for syntaxin binding, GST-syntaxin 2 (C-terminal domain, residues 181–264; Edwardson et al., 1997) was bound to glutathione-Sepharose™ (Cytiva), and the beads were incubated with purified syncollin-Strep for 3 hr at 4°C. The supernatant was removed for analysis, and the beads were washed with 10 bed volumes of 4-(2-hydroxyethyl)-1-piperazineethanesulfonic acid- (HEPES)-buffered saline, pH 7.6 (HBS). A sample of the beads was then taken, and the bound GST-syntaxin 2 was eluted with HBS containing 15 mM reduced glutathione. Syncollin in the bound, unbound and eluted fractions was detected using SDS-PAGE followed by immunoblotting, using a polyclonal anti-syncollin antibody. As a negative control, GST was attached to the glutathione-Sepharose™ in place of syntaxin 2.

4.4 | Circular dichroism spectroscopy

Syncollin-Strep was purified in 10 mM sodium phosphate, pH 8.0, containing 0.1% (w/v) CHAPS, and diluted to 10 µM in the same buffer, before 300 µl was added to a quartz cuvette for analysis using a circular dichroism (CD) spectrophotometer (Applied Photophysics). Far-UV CD data were collected between 200 and 280 nm using a 1-mm path length and a 2-nm bandwidth. A temperature ramp (25 to 95°C) was applied, with 0.5 s per point. All readings were corrected for the signal with buffer alone.

4.5 | Peptidoglycan binding

Syncollin-Strep (100 μ l of a 0.33 mg/ml solution in 10 mM sodium phosphate, pH 8.0 containing 0.1% [w/v] CHAPS) was incubated overnight at 4°C, with agitation, with or without 320 μ g insoluble peptidoglycan (Sigma). Peptidoglycan was precipitated by centrifugation at 21,000g for 3 min at 4°C. The supernatants were retained, and the peptidoglycan pellets were washed twice with ice-cold HBS. Supernatants and pellets were resuspended in equal volumes of sample buffer and analysed by SDS-PAGE followed by immunoblotting, using a polyclonal anti-syncollin antibody. As a control, bovine serum albumin (BSA) was used at the same concentration as syncollin in the binding assay and visualised on gels by Coomassie Blue staining.

4.6 | Bacterial growth curves

Lactococcus lactis (Gram-positive) and *Escherichia coli* (Gram-negative) were used to test for a potential antibacterial effect of syncollin. *L. lactis* was grown in M17 media containing 0.5% (w/v) glucose under anaerobic conditions at 30°C. *E. coli* was grown in LB broth, at 37°C, with shaking at 220 rpm. Bacteria were inoculated from glycerol stocks, and cultures were grown for 8 hr until an optical density (OD) of \sim 0.5 was reached. Bacterial growth curves were generated by quantification of absorbance using a plate reader. A 96-well format was used with a final volume of 100 μ l per well. Syncollin-Strep (or soybean trypsin inhibitor or ribonuclease A as control proteins), at various concentrations, were added in a 50- μ l volume to bacteria diluted to OD 0.01 and 0.02 for *E. coli* and *L. lactis*, respectively. Growth conditions were as described above. Negative controls (syncollin elution buffer: 10 mM sodium phosphate, pH 8.0 containing 0.1% [w/v] CHAPS and 50 mM biotin) and positive controls (40 mg/ml ampicillin) were included in all assays. OD was measured at 600 nm (for *L. lactis*) and at 660 nm (for *E. coli*). Plates were read every 30 min over a 20-hr period. Wells around the perimeter of the plates were not used, and lids were left on the plates throughout to prevent evaporation.

Ampicillin and tetracycline were used together with syncollin-Strep to investigate the effects of combination treatment. Antibiotic concentrations were selected such that bacterial growth occurred but at a reduced rate compared with control; the ampicillin and tetracycline concentrations chosen were 0.05 and 2 μ g/ml, respectively. In these experiments, syncollin was used at final concentration of 110 μ g/ml.

Each condition was represented by multiple replicates in individual experiments, with independent repeats, and plate layouts were changed in these repeats to rule out plate bias. Raw OD values were corrected for the value at time zero, so that all growth curves started at zero OD. The mean OD value in the plateau phase of growth in the control (buffer-treated) curve was taken as 100% growth, and all other data were expressed as a percentage of this value. Nonlinear regression (four parameters) was applied to generate growth curves using GraphPad Prism™. The bottom of the curve was set to zero, and Hill slopes were constrained to $<$ 0.1 in order to

eliminate ambiguous fits. Three growth parameters were derived from each curve: T_{50} , the time taken for the curve to reach half of its maximal OD; span, a measure of the increase in OD over the course of the curve, and Hill slope, a measure of the slope of the log phase of the curve. Data from independent experiments were combined. Statistical analysis used one-way ANOVA with Dunnett's or Tukey's multiple comparisons, as appropriate.

4.7 | Bacterial viability assay

Bacteria were inoculated from glycerol stocks into 5 ml of appropriate media (see above) for overnight culture. Bacteria were then diluted to OD 0.01 and incubated under various conditions: buffer alone [control] (5 mM sodium phosphate, pH 8.0 containing 0.05% [w/v] CHAPS, 25 mM biotin and complete protease inhibitors), or 300 μ g/ml syncollin, 0.05 μ g/ml ampicillin and 2 μ g/ml tetracycline in the same buffer. OD was monitored at either 600 nm (*L. lactis*) or 660 nm (*E. coli*) until bacteria reached the early plateau phase of growth (OD \sim 0.35 for *L. lactis* and 2.2 for *E. coli*). Bacteria were collected by centrifugation at 1,000g for 2 min. Bacterial pellets were washed once with phosphate-buffered saline, pH 7.4 (PBS) before resuspension in PBS containing 1 μ g/ml propidium iodide and 1 μ g/ml DAPI. Resuspended bacteria were incubated in the dark for 20 min at room temperature and then added to poly-L-lysine coated 18-well flat imaging plates (Ibidi) before confocal imaging.

Confocal imaging settings were identical for all conditions for each bacterial strain. Raw images were incorporated into image composites using ImageJ™. Brightness was adjusted identically for all images within an experiment so that red and blue staining could be clearly identified. Red staining and red plus blue staining was quantified using set colour thresholding and area measurement using ImageJ. The percentage of red (dead) cells relative to red plus blue (total) cells were then calculated. For each experiment, at least three images were analysed, and a mean percentage dead cells was determined. Data from independent experiments were then combined. Statistical analysis used one-way ANOVA with Dunnett's multiple comparisons with buffer control.

4.8 | Scanning electron microscopy imaging of syncollin-treated bacteria

Lactococcus lactis and *Escherichia coli* were incubated with syncollin-Strep, or either soybean trypsin inhibitor or ribonuclease A as control proteins, as described above. For *L. lactis*, 13-mm coverslips were washed with acetone for 5 min before coating with a 50:1 (v/w) acetone:Vectabond™ solution for 5 min. For *E. coli*, coverslips were washed with water before coating with 0.1% (w/v) poly-L-lysine (Sigma) for 30 min at room temperature. Once coated, coverslips were washed three times with water and dried in a stream of nitrogen. Bacteria in the plateau phase of their growth curves were allowed to adhere to coated coverslips for 30 min at room temperature. Coverslips were very briefly dipped twice in cold, de-ionised water to

remove any buffer salts and then quickly plunge-frozen by dipping into liquid nitrogen-cooled ethane. Samples were transferred to liquid nitrogen-cooled brass inserts and freeze-dried overnight in a liquid nitrogen-cooled turbo freeze-drier (Quorum K775X). Samples were mounted on aluminium SEM stubs using conductive silver paint (TAAB) and sputter-coated with 20-nm gold using a Quorum K575X sputter coater. Samples were viewed using an FEI Verios 460 scanning electron microscope run at 1 keV and 25 pA probe current. Images were acquired in SE-mode using an Everhard-Thornley detector.

ACKNOWLEDGEMENTS

We are grateful to Karin Muller of the Cambridge Advanced Imaging centre for her help with the SEM imaging, to Mekdes Debela of the Department of Biochemistry, University of Cambridge for the Strep tagging vector, and to the following members of the Department of Pharmacology, University of Cambridge: Marie Synakewicz, Rohan Eapen, Pam Rowling and other members of the Laura Itzhaki laboratory for help with the purification of syncollin, Sagar Raturi and Rik van Veen for help with the bacterial growth assays and Rachel Lee and Sophie Wainwright of the Edwardson laboratory for technical assistance. R.A.W. is supported by an AstraZeneca Graduate Studentship and a David James Studentship from the Department of Pharmacology.

CONFLICT OF INTEREST

The authors declare that they have no conflict of interest regarding the contents of this article.

AUTHOR CONTRIBUTIONS

James Robinson and J. Michael Edwardson: Designed the study.
Rosie A. Waters: Conducted the experiments and analysed the data.
 All three authors wrote the manuscript.

DATA AVAILABILITY STATEMENT

Data supporting the findings of this study are available from the corresponding author upon reasonable request.

ORCID

J. Michael Edwardson  <https://orcid.org/0000-0003-0499-7795>

REFERENCES

- An, S. J., Hansen, N. J., Hodel, A., Jahn, R., & Edwardson, J. M. (2000). Analysis of the association of syncollin with the membrane of the pancreatic zymogen granule. *Journal of Biological Chemistry*, 275, 11306–11311.
- Bach, J. -P., Borta, H., Ackermann, W., Faust, F., Borchers, O., & Schrader, M. (2006). The secretory granule protein syncollin localizes to HL-60 cells and neutrophils. *Journal of Histochemistry and Cytochemistry*, 54, 877–888.
- Edwardson, J. M., An, S., & Jahn, R. (1997). The secretory granule protein syncollin binds to syntaxin in a Ca²⁺-sensitive manner. *Cell*, 90, 325–333.
- Fukushima, K., Funayama, Y., Ogawa, H., Takahashi, K. I., & Sasaki, I. (2003). Decreased expression of syncollin mRNA in colonic epithelial cells of bacteria-challenged germ-free mice and ulcerative colitis. *Gastroenterology*, 124, A329.
- Geisse, N. A., Wäsle, B., Saslowsky, D. E., Henderson, R. M., & Edwardson, J. M. (2002). Syncollin homo-oligomers associate with lipid bilayers in the form of doughnut-shaped structures. *Journal of Membrane Biology*, 189, 83–92.
- Hodel, A., & Edwardson, J. M. (2000). Targeting of the zymogen-granule protein syncollin in AR42J and AtT-20 cells. *Biochemical Journal*, 350, 637–643.
- Kalus, I., Hodel, A., Koch, A., Kleene, R., Edwardson, J. M., & Schrader, M. (2002). Interaction of syncollin with GP-2, the major membrane protein of pancreatic zymogen granules, and association with lipid microdomains. *Biochemical Journal*, 362, 433–442.
- Kanagawa, M., Satoh, T., Ikeda, A., Nakano, Y., Yagi, H., Kato, K., ... Yamaguchi, Y. (2011). Crystal structures of human secretory proteins ZG16p and ZG16b reveal a Jacalin-related β-prism fold. *Biochemical and Biophysical Research Communications*, 404, 201–205.
- Li, X., Gao, Y., Yang, M., Zhao, Q., Wang, G., Yang, Y. M., ... Zhang, Y. (2014). Identification of gene expression changes from colitis to CRC in the mouse CAC model. *PLoS One*, 9, e95347.
- Makawita, S., Dimitromanolakis, A., Soosaipillai, A., Soleas, I., Chan, A., Gallinger, S., ... Diamandis, E. P. (2013). Validation of four candidate pancreatic cancer serological biomarkers that improve the performance of CA19.9. *BMC Cancer*, 13, 404. <https://doi.org/10.1186/1471-2407-13-404>
- Makawita, S., Smith, C., Batruch, I., Zheng, Y., Rückert, F., Grützmann, R., ... Diamandis, E. P. (2011). Integrated proteomic profiling of cell line conditioned media and pancreatic juice for the identification of pancreatic cancer biomarkers. *Molecular and Cellular Proteomics*, 10, M111.008599. <https://doi.org/10.1074/mcp.M111.008599>
- Min, H. J., Yun, H., Ji, S., Rajasekaran, G., Kim, J. I., Kim, J. S., ... Lee, C. W. (2017). Rattusin structure reveals a novel defensin scaffold formed by intermolecular disulfide exchanges. *Scientific Reports*, 7, 45282.
- Mukherjee, S., Zheng, H., Derebe, M. G., Callenberg, K. M., Partch, C. L., Rollins, D., ... Hooper, L. V. (2014). Antibacterial membrane attack by a pore-forming intestinal C-type lectin. *Nature*, 505, 103–107.
- Murashko, O. N., & Lin-Chao, S. (2017). *Escherichia coli* responds to environmental changes using enolase degradosomes and stabilized DicF sRNA to alter cellular morphology. *Proceedings of the National Academy of Sciences of the United States of America*, 114, E8025–E8034.
- Rubinstein, E., Mark, Z., Haspel, J., Ben-Ari, G., Dreznik, Z., Mirelman, D., & Tadmor, A. (1985). Antibacterial activity of the pancreatic fluid. *Gastroenterology*, 88, 927–932.
- Shin, J. H., & Seeley, R. J. (2019). Reg3 proteins as gut hormones? *Endocrinology*, 160, 1506–1514.
- Tan, S., & Hooi, S. C. (2000). Syncollin is differentially expressed in rat proximal small intestine and regulated by feeding behavior. *The American Journal of Physiology*, 278, G308–G320.
- Wäsle, B., Hays, L. B., Rhodes, C. J., & Edwardson, J. M. (2004). Syncollin inhibits regulated corticotropin secretion from AtT-20 cells through a reduction in the secretory vesicle population. *Biochemical Journal*, 380, 897–905.
- Wäsle, B., Turvey, M., Larina, O., Thorn, P., Skepper, J., Morton, A. J., & Edwardson, J. M. (2005). Syncollin is required for efficient zymogen granule exocytosis. *Biochemical Journal*, 385, 721–727.

SUPPORTING INFORMATION

Additional supporting information may be found online in the Supporting Information section at the end of this article.

How to cite this article: Waters, R. A., Robinson, J., & Edwardson, J. M. (2021). Syncollin is an antibacterial polypeptide. *Cellular Microbiology*, e13372. <https://doi.org/10.1111/cmi.13372>